Jour. Fac. Sci., Hokkaido Univ., Ser. VII (Geophysics), Vol. 11, No. 1, 89-115, 1998.

An Observational Study on the Generation and Development of Meso-β and γ Scale Band Clouds in Winter around Rebun Island, Hokkaido, Japan

Akio Takemoto*, Hiroshi Uyeda, Katsuhiro Kikuchi and Naonori Osaki

Division of Earth and Planetary Sciences, Graduate School of Science, Hokkaido University, Sapporo 060-0810, Japan

(Received November 30, 1997)

Abstract

We carried out observations of snow clouds in Rebun Island which is located in the northern Japan Sea about 60 km west of the west coast of Hokkaido Island, utilizing a dual-linear-polarization Doppler radar, radiosondes and other facilities from January 16 to 28, 1991. The purpose of the observations was to reveal formation mechanism of convective clouds, which produce heavy snowfalls around the west coast of Hokkaido Island during the winter monsoon season. Four snowfall events were observed around Rebun Island during this observation period. A long lasting and active broad band cloud observed from January 22 to 23 in 1991 was analyzed in detail. The band cloud was generated along the horizontal shear line between a northeasterly flow blowing from the Soya Strait and the northwesterly monsoon over the west of Soya Strait. The northeasterly flow was shallow (the depth was <1 km) and colder than the northwesterly flow by 1°C, and it had the same structure as a gravity current. The northwesterly flow was forcibly lifted into a convective unstable layer (at the height of 1.0-2.7 km) by the northeasterly wind. A strong updraft (up to 5 m/s) was generated just ahead of the northeasterly flow due to the strong convergence, which resulted in generating strong convective cells successively along the shear line. Kelvin-Helmholtz instability was generated within the vertical shear layer (at the height of 0.5-1.5 km) in the east of the strong convective cells, and it resulted in rotors with a diameter of 2 km there. The generating and developing mechanisms of the northeasterly flow is discussed.

1. Introduction

Many meteorological observations have been carried out along the west coast of the Hokkaido Island during wintertime to study the formation mecha-

* Present affiliation: Environment Agency of Japan 1-2-2 Kasumigaseki, Tokyo 100-0013, Japan.

nism of band clouds. Band clouds are usually generated over the Japan Sea, such as off the west coast of Hokkaido Island (Kobayashi et al. (1988); Nagata and Ikawa (1988); Tsuboki et al. (1989); Uyeda et al. (1991); Ninomiya et al. (1993) etc.) and off the east coast of the Korean Peninsula (Nagata et al. (1986); Research group on mesoscale meteorology of Marine Department, JMA (1988) (hereafter referred as JMA (1988)); Ishihara et al. (1989); Nagata (1992); Nagata (1993) etc.). Band clouds bring heavy snowfalls over the areas as they reach, and are sometimes associated with vortex like meso low pressure systems.

Band clouds have a few other different names according to authors. For example, they were called convergence band clouds (CBCs) by Kobayashi et al. (1988), or convergence cloud bands (CCBs) by Nagata (1992). Usually, these names are distinguished by the scale of cloud system. If they are defined as meso-α disturbances (Nagata and Ikawa (1988); Nagata (1992) etc.), they are called cloud bands. Developed cloud bands observed over the northern Japan Sea by GMS (Geostationary Meteorological Satellite) have 20-50 km in width, 200-300 km in length and 4-5 km in height, and these time scales are more than a day. A cloud band comprises several band-shape clouds. They are usually called band clouds. Band clouds are usually classified as Meso-β scale disturbances. They are observed with Doppler radars (Tsuboki et al. (1989); Uyeda et al. (1991) etc.). In the present paper, we simply use the expression "band clouds" in order to avoid the confusion by giving a certain name before revealing their internal structure and formation mechanism.

A number of studies on cloud bands of the northern Japan Sea have been carried out. Okabayashi and Satomi (1971) proved the existence of cloud bands by analyzing GMS images. Kibe (1988) classified meso-scale disturbances with the shapes of images and the longevities, and described each typical synoptic scale feature. Kobayashi et al. (1987) performed meso-scale analyses by using T_{BB} of GMS and AMeDAS (Automated Meteorological Data Acquisition System) data etc. They explained that convergence band clouds (CBCs) observed off the west coast of Hokkaido are characterized by a convex line toward the west over the west of the Soya Strait. They also explained that a land breeze which is caused by a high pressure system over inland Hokkaido plays an important role in generating and maintaining CBCs.

Tsuboki et al. (1989) analyzed a convergence band cloud which advanced into the Ishikari bay from the inland Hokkaido based on Doppler radar observations. They concluded that the motion of the convergence band cloud corresponded to a land breeze, and that the land breeze front was geometrically and

dynamically similar to that of a gravity current.

Observations of band clouds in Hokuriku district have been also carried out by several researchers. For example, Ishihara et al. (1989) studied the dynamic mechanism of snow bands which generated parallel to the west coast of the Hokuriku district. They also pointed out the importance of a land breeze in the formation of clouds parallel to the coast line.

As well as observational studies using such instruments as Doppler radars and radiosondes described above, numerical simulations to study the dynamic and thermodynamic structure of cloud bands have been carried out. Nagata and Ikawa (1988) made numerical experiments on convergence clound bands (CCBs) which generated in the west coast of Hokkaido Island, and concluded that the thermal contrast between the Korean peninsula and the Japan Sea play an important role in generating and maintaining CCBs. Tsuboki and Wakahama (1992) carried out data analyses of observations and linear instability analysis on mesoscale cyclones accompanied by convergence band clouds off the west coast of Hokkaido Island. They concluded that the mesoscale cyclones are baroclinic instability disturbances developing in a particular baroclinic flow.

Band clouds observed around Ishikari Bay, where radar observation network has been completed, are modified by the orographic effect. In order to study the formation mechanism of band clouds less modified by the orographic effect, we have to choose a site for observations far from Hokkaido Island, such as Rebun Island. However, in terms of observations of band cloud around Rebun Island, only satellite or radiosonde observations were carried out before, and no radar-based observation has been done. Therfore we carried out observations with dual-linear-polarization Doppler radar (Faculty of Science, Hokkaido University) at Rebun Island from January 16 to 28, 1991. This period was selected because developed band clouds are often observed over the Japan Sea during the latter half of January.

Four snowfall events were observed during this observation period. In this paper, a band cloud which was observed within the radar range in the second event were studied. We made analyses of the kinematic, dynamic and thermodynamic structure of the band cloud by using the meteorological data from the Doppler radar, radiosondes and ground observation.

2. Method

2.1 Observation

Figure 1 shows maps around the observational site of Rebun Island.

Observations were carried out at the northern cape of Rebun Island (45°28′N, 40° 58′E). Rebun Island is located in the Japan Sea about 60 km away from the west coast of Hokkaido Island.

The site is a suitable place to observe band clouds without the modification of orographic effects during winter monsoon surges, since it is located in the ocean about 60 km west from the west coast of Hokkaido Island. Within the radar observation range from Rebun Island is known as the area of initiation of

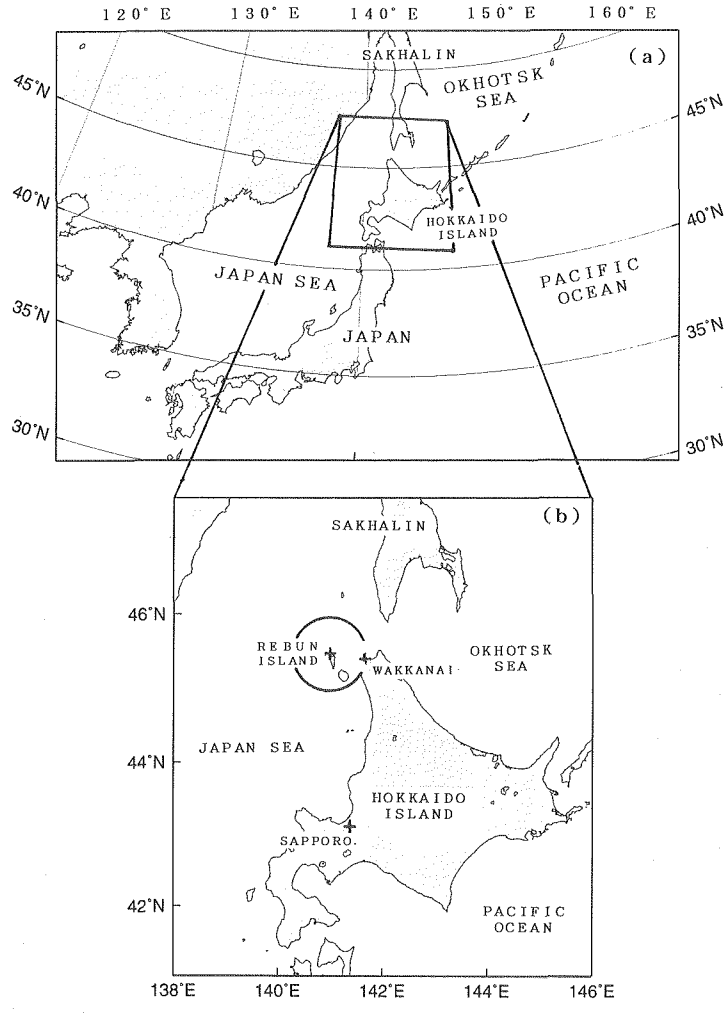

Fig. 1. (a) A map around Japan. (b) A map around Rebun Island, Hokkaido, Japan. The circle shows the range of radar observation ($r=60$ km).

long lasting and active band clouds in winter, as suggested by Kobayashi et al. (1987) and others.

Kinematic and internal structures of convective snow clouds were observed with a dual-linear-polarization Doppler radar (λ(wave length)=3.2 cm). The specification of the radar is described by Uyeda et al. (1991). The observation data with the Doppler radar mode was used. The elevation angles of PPI scans ranged from 0° to 9°, since only low elevation scans were required for the observation of shallow snow clouds below 4 km in height. The PPI and RHI data was collected in 15-20 minute intervals.

Radiosonde and surface weather data were collected at the radar site. Soundings by Wakkanai Meteorological Observatory were utilized for the analyses. Satellite data from GMS and NOAA-10, and maritime meteorological data off the west coast of Hokkaido Island by Keifu-maru of the Japan Meteorological Agency were also utilized in the analysis.

Observations were carried out from January 16 to 28, 1991. Especially, in the latter half of this period, several types of cloud bands were observed within the radar observation range (r=60 km).

2.2 Analyses

a) Velocity-Azimuth Display (VAD)

The method of VAD is one of the analytic ways to determine the vertical profile of a linear wind field using a single Doppler Radar, and was introduced by Browning and Wexler (1968) and others. We consider that the wind field and precipitaion fall speed are horizontally homogeneous. As the radar beam rotates around a vertical axis at a fixed elevation, the mean radial velocity is given by a sine function of azimuth angle.

Browning and Wexler (1968) approximated this sine function by harmonic functions. Divergence is obtained from the magnitude of the "zeroth" harmonic when the vertical component of a linear wind field is neglected, the wind speed and direction is obtained from the amplitude and phase of the fundamental, and deformation and the orientation of the axis of dilatation is obtained from the amplitude and phase of the second harmonic.

Tsuboki and Wakahama (1988) obtained the coefficient of each harmonic by using method of least squares. This method was adopted in this paper for the analysis of horizontal wind. Doppler velocities which were more than Nyquist velocity (±12 m/s) were dealiased considering the continuity of horizontal wind. The fall speed of precipitation particles was assumed to be 1 m/s since the majority of the precipitation particles observed were snowflakes. The assump-

tion makes the maximum errors of the wind speed less than 0.2 m/s. The vertical profile of horizontal wind field was obtained continuously since the radial velocity was recorded at every range gate. The range gate interval was 250 m in the present Doppler radar observation.

b) Volume Velocity Processing (VVP)

The method of VVP is one of the most useful ways, which was first introduced by Waldteufel and Corbin (1979), to obtain kinematic properties of a linear wind for single Doppler radar data by using the theory of multivariate regression. When a detailed horizontal distribution of a wind field in the lower layer is needed, the sector VAD method at a low elevation angle is known to be useful for widespread uniform clouds. But in the case of narrow cloud bands or isolated clouds, wind fields contain large errors due to the lack of velocity data in a sector plane. On the other hand, the VVP use a lot of data (1,000-5,000) in the analysis volume of two adjacent elevation angles. So the VVP is a useful way to obtain kinematic fields (wind, divergence, deformation, etc.) of narrow cloud bands in detail.

We simplified the VVP method by Koscielny et al. (1982) to obtain the mean wind field in the analysis volume. Their method is as follows.

First we assume the measurement point (r, θ, ϕ ; r is range, θ is elevation, ϕ is azimuth) in the spherical earth coordinate system. This point is also expressed by the Cartesian coordinate system (x, y, z). The wind velocity vector $\boldsymbol{v}$ at (r, θ, ϕ) was assumed to be well represented by a first-order (linear) Taylor series in the analysis volume.

In this analysis, Doppler velocities of the PPI at two elevation angles (1° and 2° or 2° and 3°), which were successively recorded, were used. The vertical component of the $\boldsymbol{v}$ was eliminated because it contained a large error affected by precipitation particles and because only the horizontal wind fields were of concern to us. The size of analysis volume (Δr, $\Delta\theta$, $\Delta\phi$) was $\Delta r = 15$ km, $\Delta\theta =$ 1° or 2°, $\Delta\phi = 30°$. Allocating the center of the analysis volumes (x_0, y_0) in the 5 km×5 km grid volume, we obtained the horizontal wind field in each grid volume. The amount of errors was about 1-5° in wind direction and 0.5-1.0 m/s in wind speed. These values assured the precision of this analysis.

c) Calculation of wind on RHI plane

The wind field on an RHI plane was obtained by assuming the two dimensionality. Neglecting the wind component perpendicular to this plane, a horizontal wind component in a 250 m×250 m was calculated by averaging the horizontal components of Doppler velocities in the grid. Then a horizontal divergence was calculated with the continuity equation. Finally a vertical wind

component was given by integrating the horizontal divergence toward the upward direction.

3. Results

3.1 Synoptic situation

A summary of the pressure pattern near Rebun Island and of the surface weather at the observation site is shown in Fig. 2. Four snowfall events were observed during the observation period. Two developed low-air pressure systems passed from January 17 to 18 and from January 25 to 26, which we named EVENT1 and EVENT3 respectively. The stratiform snow clouds with strong easterly wind and high equivalent potential temperature at all heights were observed around the observation site during these periods. The site was covered with a cold air mass from January 22 to 23 and from January 27 to 28 which we named EVENT2 and EVENT4 respectively. Significant convergent cloud bands were observed around the observation site during these periods. Figure 3 shows the time-height cross section of wind and equivalent potential temperature at Wakkanai from January 21 to 28, 1991. The most prominent long lasting broad band cloud was observed within the range of the Doppler radar mode during EVENT2. This event is analyzed in this paper.

Weather charts at 2100 JST (JST = UTC + 9 hours) on January 22 are shown in Fig. 4. The surface pressure pattern shows that the winter northwesterly monsoon was prominent over Japan (see Fig. 4(a)). A developed low pressure

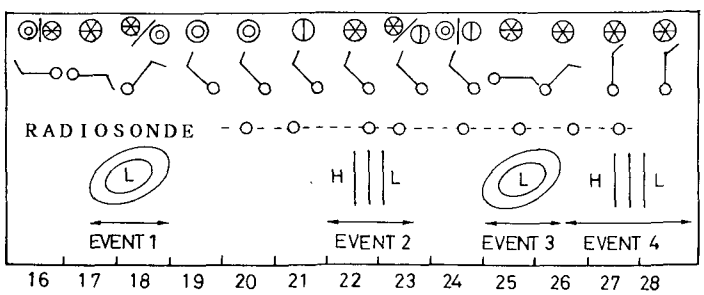

Fig. 2. A summary of observations at Rebun Island. Weather (top line, ⓓ: clear, ◎: cloudy, ⊗: snowy, | : sometimes, / : later), wind directions (second line), radiosonde release time (third line) and sea surface pressure patterns (fourth line) from January 16 to 28, 1991 are indicated. A developing low pressure system was located to the south of the observation site in EVENT1 and EVENT3, and a typical winter air pressure pattern around Japan (low in the east and high in the west) appeared in EVENT2 and EVENT4.

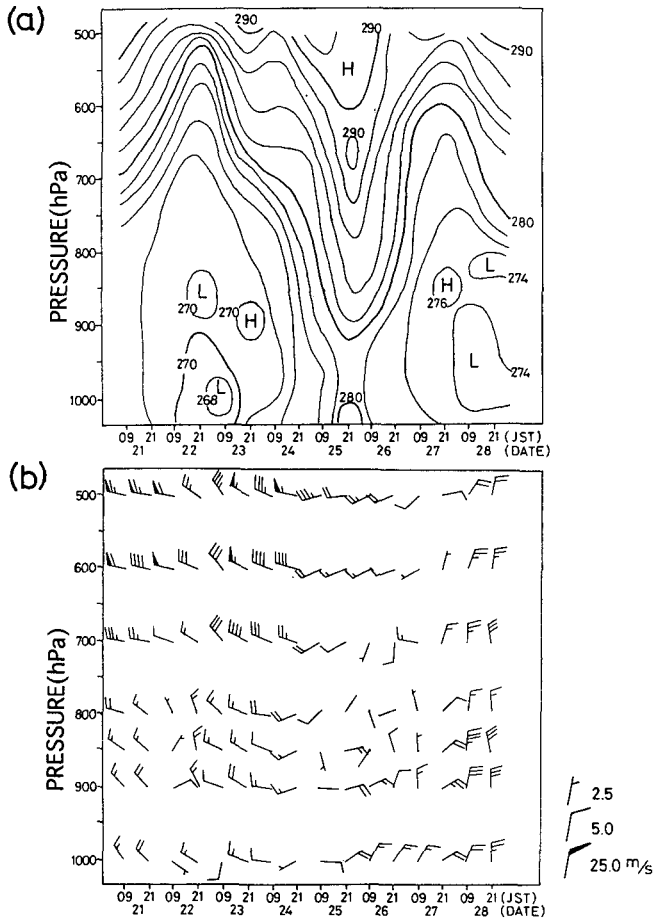

Fig. 3. Time-height cross sections of equivalent potential temperature and winds derived from serial radiosonde observation at Wakkanai from January 21 to 26, 1991. The interval of the isotherms is 1K. A half barb, a full barb and a flag indicate 2.5, 5.0 and 25 m/s respectively.

was located near Aleutian Islands, far northeast of Hokkaido Island. High pressures appeared around the north of the Korea Peninsula. The gradient of the air pressure was rather small over Hokkaido Island at that time. A significant cold air mass which was below −42°C at 500 hPa covered Hokkaido Island (not shown). Figure 4(b) shows that the air over off the west coast of Hokkaido Island was relatively warmer than that over both the western Japan Sea and off the east coast of Hokkaido Island.

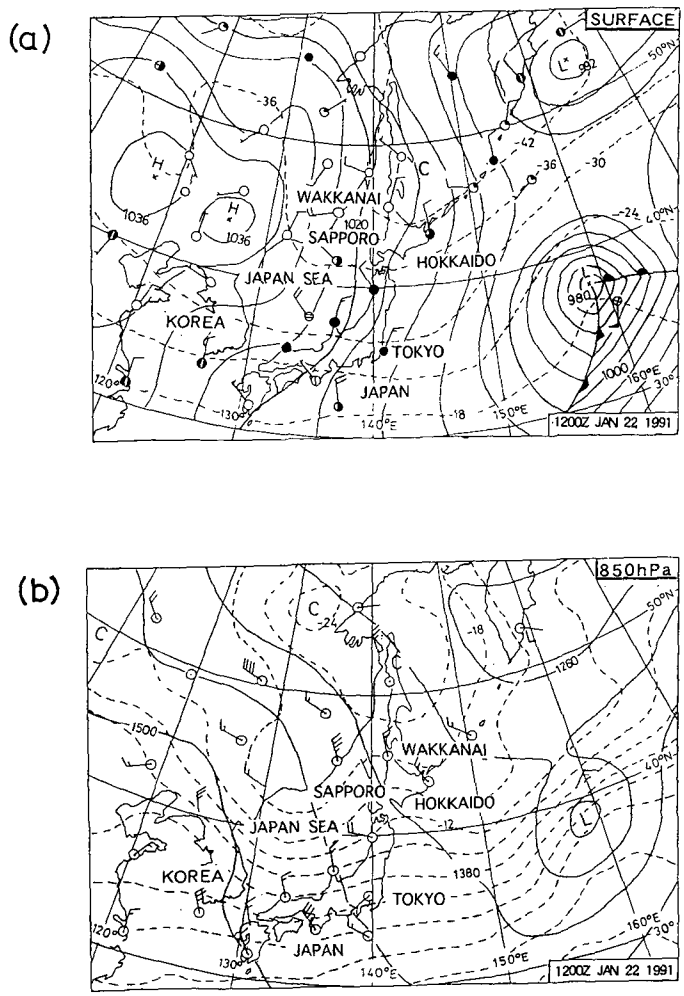

Fig. 4. Weather charts around Japan at 2100 JST on January 22, 1991. (a) sea surface pressure with 500 hPa temperature, (b) height and temperature at 850 hPa.

3.2 Kinematic structure of band cloud

Figure 5 shows the time series of the PPI radar echoes at the elevation angle of 1° at intervals of about one hour, from 2000 JST on January 22, to 0700 JST on January 23. A lot of open cell echoes were observed around Rebun Island at 2000 JST on January 22. They were moving toward southeast with the northwesterly winter monsoon. Strong echoes of a broad band cloud extending from

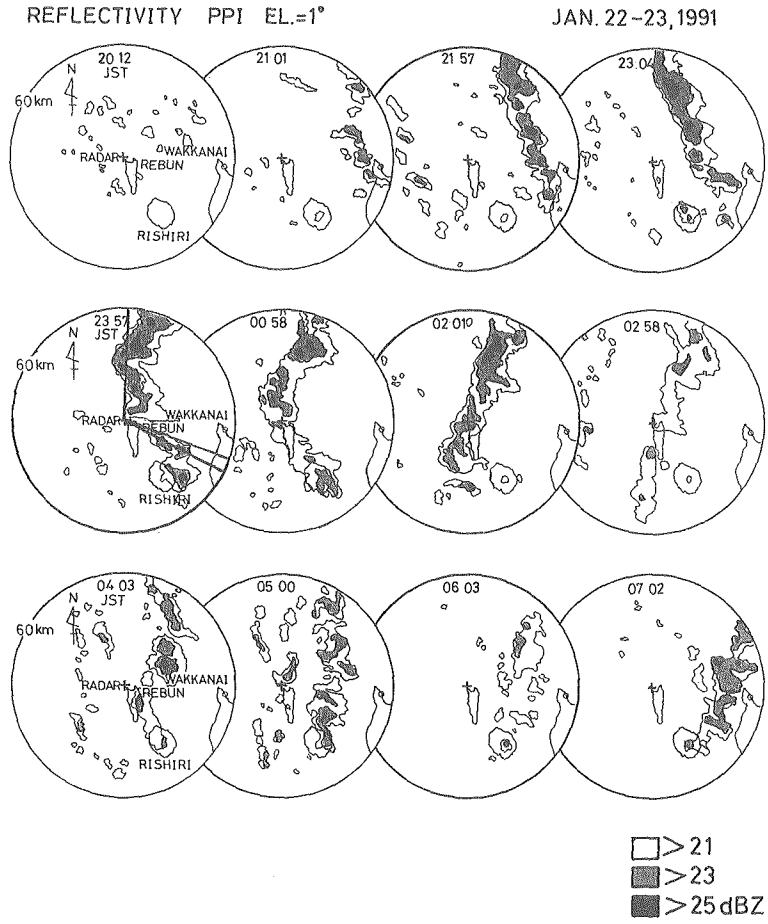

Fig. 5. Time series of the PPI radar echo patterns in EVENT2. Solid lines at 2357 JST show the directions of vertical cross sections in Fig. 10 (azimuth=2.2°) or Fig. 11 (azimuth=110.0° and 116.6°).

north-northwest (NNW) to south-southeast (SSE) moved toward the radar site from 2100 to 2400 JST. At 2357 JST, a bend of the echoes was observed. Around 0030 JST on January 23, a very strong echo passed over the radar site and soft hails were observed on the ground at 0033 JST (Fig. 6(a)). The band cloud was more than 100 km in length and more than 20 km in width at the mature stage. After 0201 JST, the echoes weakened and densely rimed snowflakes were observed there at 0215 JST (Fig. 6(b)). Then the echoes started receding to the east.

However the intensity of echoes was enhanced again around 0700 JST.

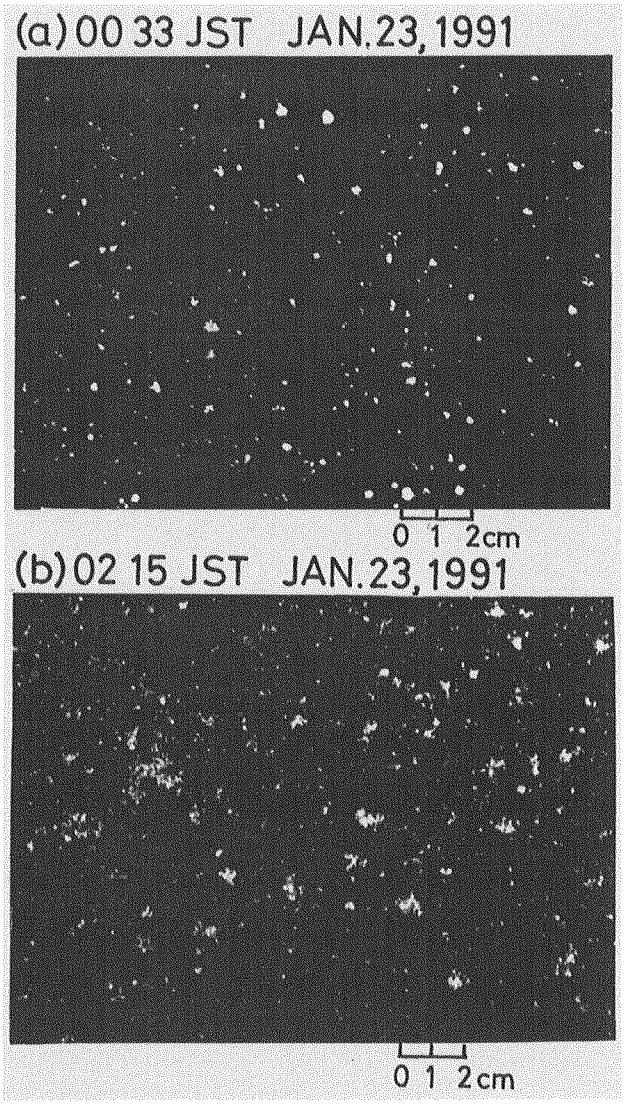

Fig. 6. Examples of snow particles collected on a board with a black velvet cloth on 23 January 1991. (a) soft hails at 0033 JST. (b) densely rimed snowflakes at 0215 JST.

The infrared imagery of NOAA/AVHRR (Fig. 7) show the signatures of a broad cloud band and band clouds (see 0702 JST in Fig. 5) at 0701 JST on January 23. As seen in Fig. 7 as cloud distribution, there were a lot of strong echoes around the west side of the band echoes, but few in the east side. Line echoes, moving

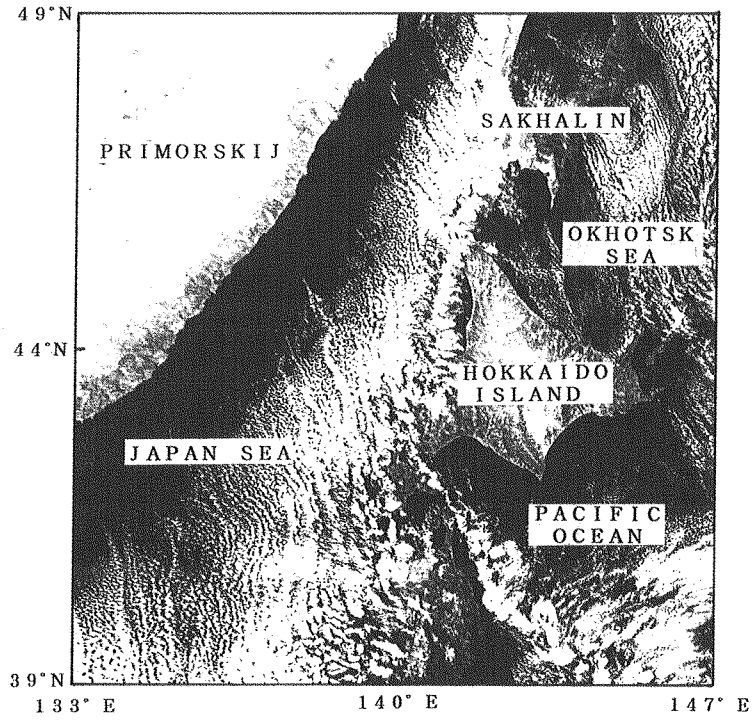

Fig. 7. Infrared image of NOAA-10 (IR CH. 4) at 0701 JST on January 23, 1991.

toward southeast with the winter monsoon, collided against the band echo at its west side. The echoes of the band cloud were growing when the band cloud was approaching the radar site. The echoes bent to the west.

In relation to the passage of the band cloud, the time series of wind and temperatures on the ground at the radar site (Rebun Island) and Wakkanai during EVENT2 is investigated (Fig. 8). As for Rebun, the wind direction was northwest (NW), temperatures changed periodically by less than 1.5°C until 0000 JST January 23. It is considered that these results corresponded to the passing of streak clouds elongating from northwest to southeast with the northwesterly winter monsoon. Just after the time when the head of the band cloud passed the radar site around 0020 JST, the surface temperature decreased about 1°C and the wind direction shifted drastically from northwest (NW) to northeast (NE) there. The wind speed of the NE wind was slower than that of the NW (7 m/s) wind by a few meters per second. The temperature began rising at 0130 JST. The wind direction began turning from NE to NW at 0300 JST. At 0330

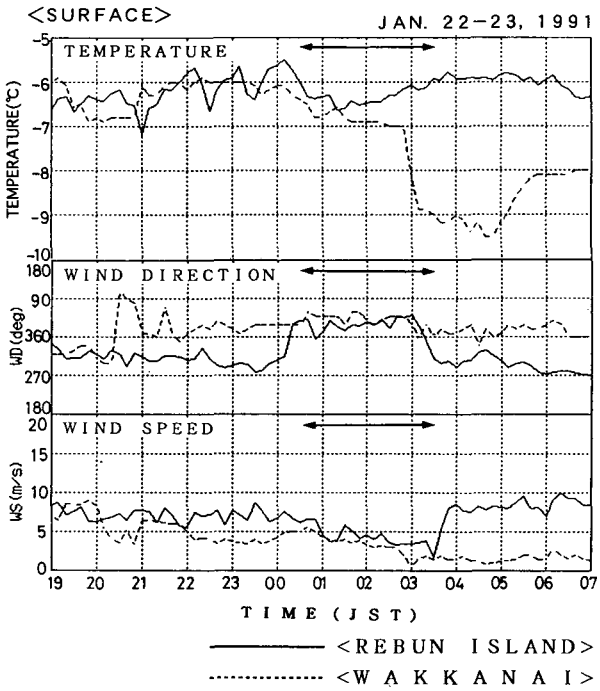

Fig. 8. Time series of the temperature, wind direction and wind speed on the ground in EVENT2. Solid lines indicate data observed at Rebun Island and dashed lines indicate Wakkanai meteorological observatory's data. Arrows show the period when the band cloud was prominent over Rebun Island.

JST the wind direction shifted back to NW and the wind speed began increasing. By 0400 JST the wind speed increased by 6 m/s. As for Wakkanai, the temperature began decreasing at 1930 JST. Then the wind direction shifted from NW to east (E) drastically and the wind speed decreased by about 3 m/s at 2030 JST. Around 0300 JST, the wind direction shifted from NE to north (N) and the wind speed changed from 4 m/s to 1 m/s. The temperature decreased by 2°C at the same time. It is considered that a cooler air advected from the inland Hokkaido to Wakkanai since NE wind weakened there. Compared Rebun Island to Wakkanai, the temperature and wind from 0030 JST to 0320 JST in Rebun Island was nearly equal to that in Wakkanai.

The time-height cross section of the horizontal wind (Fig. 9) obtained by using the VAD method at Rebun Island during EVENT2 shows one of the characteristics of the band cloud. From 0100 JST to 0300 JST on January 23, there was a weak northeasterly wind not more than 5 m/s below the altitude of

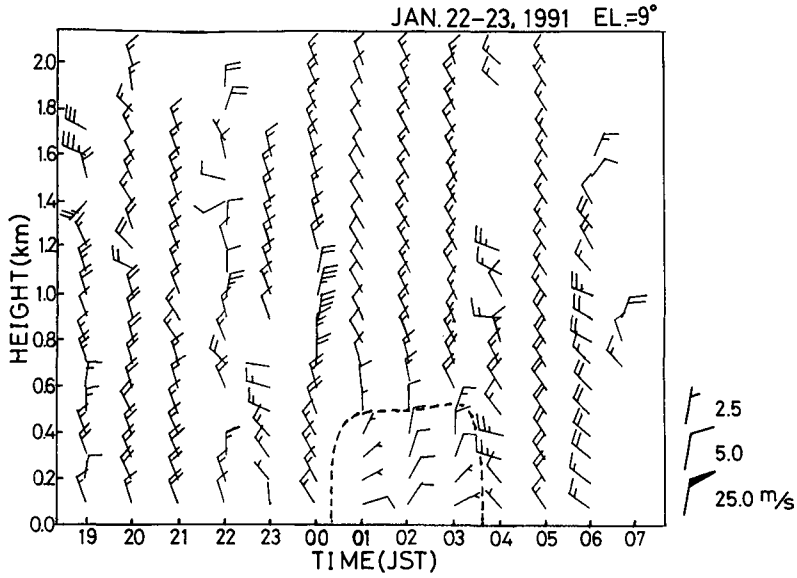

Fig. 9. Time-height cross section of winds derived from VAD at 9° elevation angle. Dashed line shows the domain where the northeasterly flow intruded over the radar site.

600 m over the radar site. These results indicate that the cold and shallow northeasterly flow composed the east part of the band cloud.

In order to see the internal structure of the cloud band, the vertical cross section of reflectivity (Azimuth=2.2°, approximately north-south section), parallel to the approaching echoes of the band cloud at 0013 JST on January 23 is shown in Fig. 10. Arrows show winds on the 250 m×250 m grids, which are calculated by assuming two dimensionality on the plane (wind vectors were omitted every other grid from the panel). The cell motion (5 m/s) is subtracted from the horizontal wind speed. Strong convective cells were lined up regularly at about 4 km intervals and the maximum height of these echoes reached up to 4 km. The vertical wind fluctuated at intervals of several kilometers. It is considered to be associated with the interval of the development of the echoes.

The time series of the vertical cross section perpendicular to the band cloud is shown in Fig. 11. The thick solid line on the echo in each panel indicates the boundary between the westerly and easterly winds. The easterly wind was observed at lower altitudes as the echoes approached the radar site. The westerly wind was lifted at the head of the easterly. There was a strong updraft just ahead of the easterly wind due to the strong convergence. The

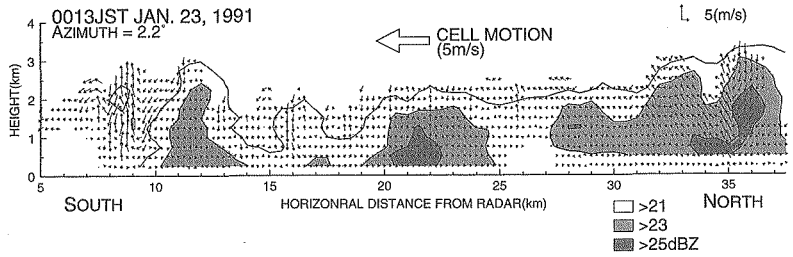

Fig. 10. Vertical cross section of reflectivity and wind field parallel to the band cloud (azimuth is 2.2°). Arrows show winds on the 250 m×250 m grids, which were calculated by assuming two dimensionality on the plane, and the cell motion (5 m/s) was subtracted. Wind vectors were omitted every other grid from the panel.

velocity of the updraft was up to 5 m/s. The strong echoes, with values of more than 23 dBZ, were located just behind the strong updraft and head of the easterly wind. These strong echoes corresponded to some of the strong ones around the west edges of the band cloud on the PPI planes in Fig. 5. A strong vertical wind shear was shown around the boundary of these two flows, at an altitude of about 1 km. To the rear of the strong updraft, there seemed to be rotors, which were about 2 km in diameter, within the shear layer at $r=21$ and 26 km (distance from the radar site) at 2348 JST. Relatively weak echoes were shown around these rotors at 2348 JST. At 0048 JST, periodic weak echoes were seen, though no rotors were obvious in the wind field. The shape of the strong echoes always inclined to the direction of the propagation of the echoes and against the direction of the vertical wind shear.

While the band cloud was staying over the Rebun Island, the pattern of the echoes kept the steady state. From these characteristics of the echoes, we assume that the internal structure of the band cloud and precipitation mechanism are as in the following description. At first, a lot of cloud water was generated in the updraft layer, then the snowflakes rimed by the cloud water grew into the soft hail just behind the updraft. Finally the soft hail fell on the ground several kilometers east of the strong updraft since it was transferred backward (to the east) by the westerly wind. On the other hand, the rimed snowflakes, which were generated in the updraft area, were transferred backward further than the soft hail due to the light smaller fall speed, so it fell on the ground more than 10 kilometers east of the strong updraft. It is concluded that the strong echoes just behind the updraft corresponded to the soft hail, and the relatively weak echoes around the rotors corresponded to the rimed

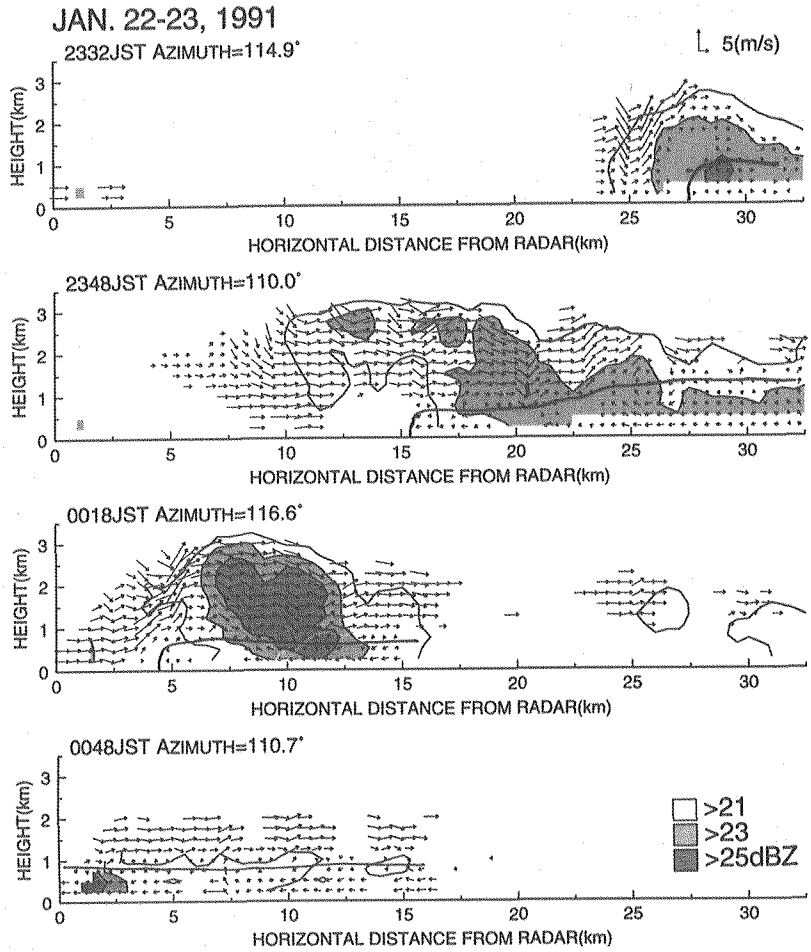

Fig. 11. Vertical cross sections of reflectivity and wind field perpendicular to the band cloud (azimuth is about 110°). Arrows show winds on the 250 m×250 m grids, which were calculated by assuming two dimensionality on the planes. A boundary between the easterly and westerly wind is drawn by a thick solid line. Wind vectors were omitted every other grid from the panels.

snowflakes. This assumption is supported by the observed snow particles as shown in Fig. 6.

The horizontal wind fields in the lower layer around the radar site obtained by the VVP method, when the band cloud was around Rebun Island, are shown in Fig. 12. At 0024 JST, when the band cloud reached the radar site, a relatively weak easterly wind (about 5 m/s) prevailed on the east side of the radar site.

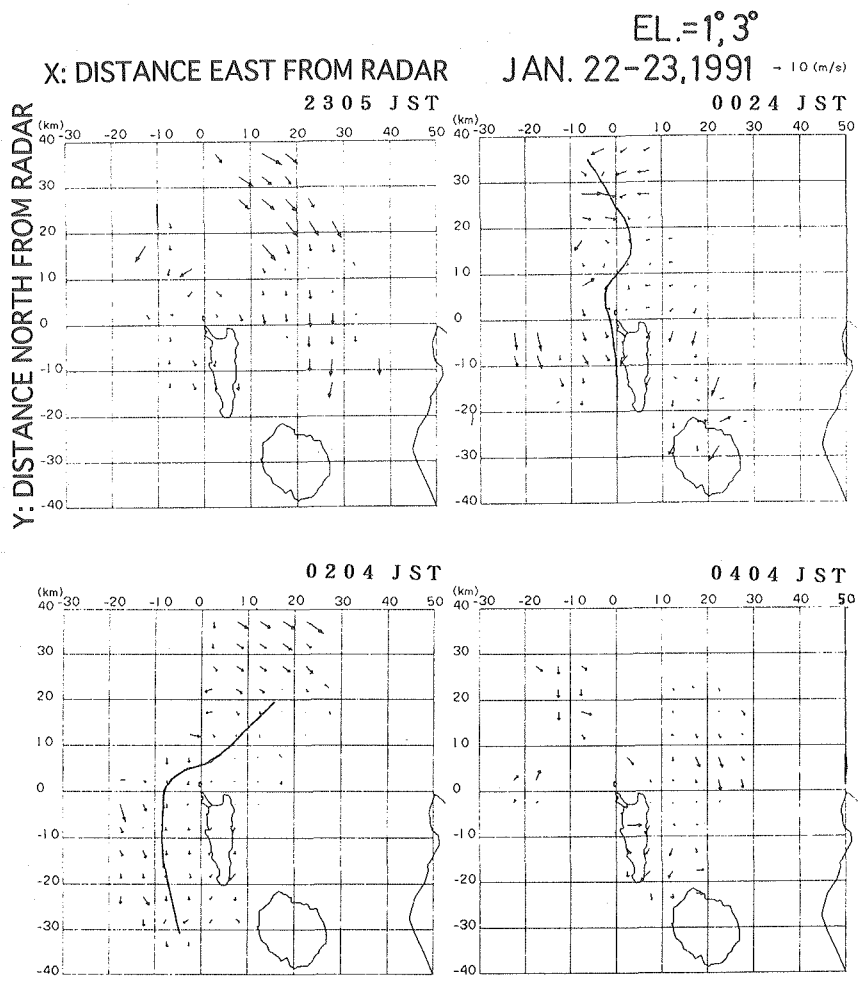

Fig. 12. Time series of horizontal winds derived from the VVP analysis in EVENT2. The solid line indicates the shear line (a boundary between the easterly and westerly wind).

So did a relatively strong northwesterly wind (above 10 m/s) on the west side. A convergence line between the easterly and the westerly wind (indicated by a solid line which we will call the shear line hereafter) is clearly seen from north to south, at the distance of about 0 km east from the radar site. At 0204 JST, the southern half of the shear line proceeded up to 10 km off the west coast of Rebun Island. Whereas the northern half of it receded toward southeast because the northeasterly flow weakened there. At 0404 JST, the shear line had

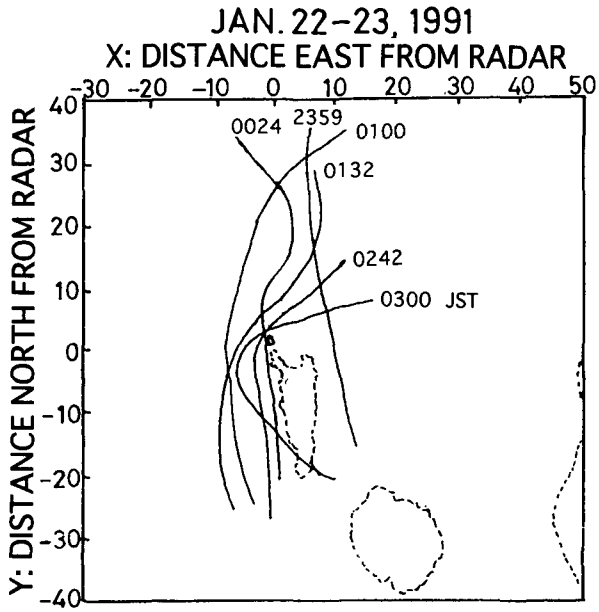

Fig. 13. The motion of the shear line around Rebun Island during EVENT2 derived from VVP analysis.

already disappeared, and a northerly wind was seen around the radar site.

The movement of the shear line from 2359 JST on January 22 to 0300 JST on January 23 is shown in Fig. 13. The shear line proceeded straight towards the west until 0024 JST, at 0100 JST it bent to the west in response to the shape of the band cloud. Then the shear line began receding toward the east in the northern area of the radar site. Finally at 0300 JST, the shear line almost completely receded except for the area above and around Rebun Island. The motion of the shear line was clearly in accordance with the band cloud's motion (see Fig. 5). When the shear line proceeded toward the west, the band cloud was developed. On the contrary, when the shear line receded toward the east, the band cloud weakened. It is thought that the motion of the shear line was determined by the balance of forces of the westerly and the easterly winds.

3.3 Thermodynamic structure of band cloud

Then we analyzed the vertical thermodynamic structure in the band cloud. Figure 14 shows vertical profiles of temperatures and wind from radiosondes launched from Rebun and Wakkanai. Soundings at 2000 JST on January 22 at Rebun, 2100 JST on January 22 and 0300 JST on January 23 at Wakkanai are

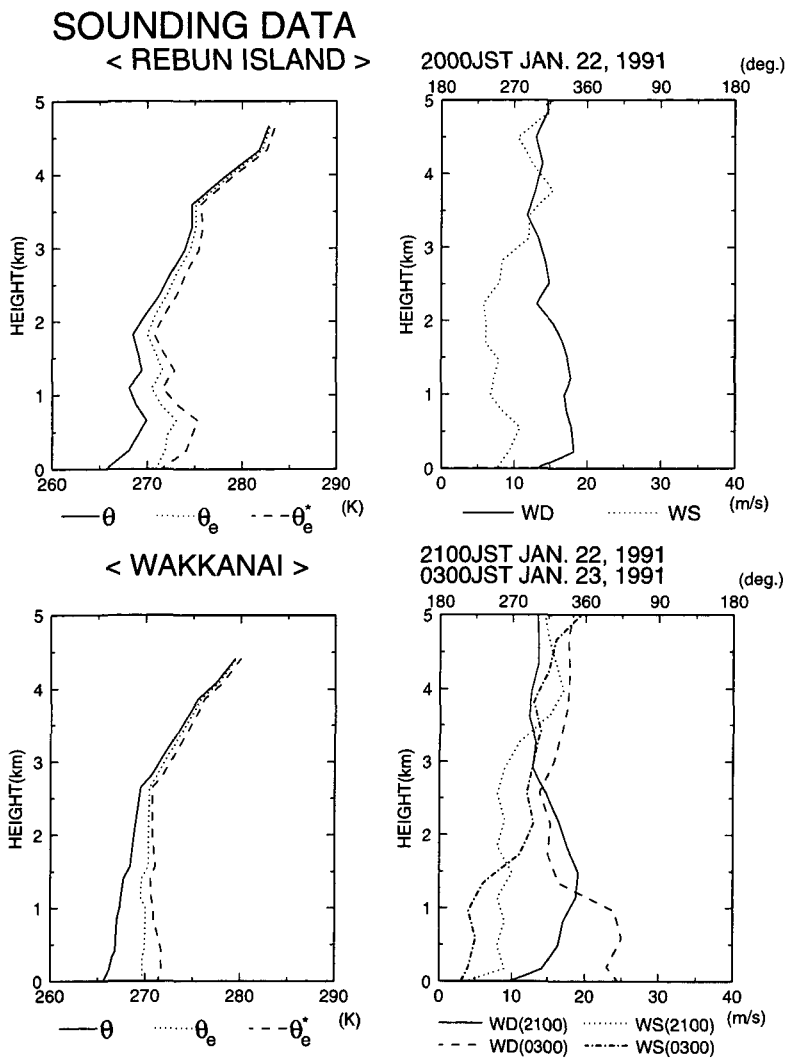

Fig. 14. Sounding curves at Rebun Island and Wakkanai in EVENT2. Data from Wakkanai was obtained by Wakkanai meteorological observatory. The upper figures show the data at Rebun Island at 2000 JST on January 22, 1991 and the lower ones show the data at Wakkanai at 2100 JST on January 22 and 0300 JST on January 23, 1991 respectively. The potential temperature (solid line), equivalent potential temperature (dotted line) and saturated equivalent potential temperature (dashed line) are shown in the left panels, the wind direction (2000 JST, 2100 JST: solid line, 0300 JST: dashed line) and wind speed (2000 JST, 2100 JST: dashed line, 0300 JST: dot dashed line) are shown in the right panels.

shown, though the temperature and humidity were not available at 0300 JST at Wakkanai.

At Rebun, the wind direction ranged from WNW to NNW at 2000 JST on January 22. The vertical wind shear was small. From the profile of equivalent potential temperature, the depth of convective mixing layer is estimated to be 1.8 km. The convective instability is calculated with the gradient of saturated equivalent potential temperature. There were stable layers below the height of 0.6 km, from 1.1 km to 1.3 km and above 1.8 km. On the other hand, there were two unstable layers from the height of 0.6 km to 1.1 km and from 1.3 km to 1.8 km.

At Wakkanai, the wind direction was west on the ground and gradually turned to north up to the height of 1.5 km at 2100 JST on January 22. The wind speed was constant at about 8 m/s below the height of 3 km. The depth of convective mixing layer is estimated to be 2.6 km. And there was a convectively stable layer above 2.6 km. At 0300 JST, the wind direction shows that the weak (<5 m/s) northeasterly wind prevailed below the height of 1 km. It is estimated that the cold northeasterly flow in the lower layer, which consisted of the band cloud, was prominent over Wakkanai.

4. Discussion

4.1 Dynamic structure of northeasterly flow

Now we discuss the characteristics of the northeasterly flow which plays an important role on the formation of the band cloud. Tsuboki et al. (1989) pointed out that a land-breeze front, which is formed by a cold outflow on the inland of Hokkaido, plays an important role on the formation and maintenance of a convergence band cloud, and that the front was geometrically and dynamically similar to that of a gravity current found in laboratory experiments. They also suggested that the structure of the gravity current was similar to that of a thunderstorm outflow.

Simpson (1987) showed the conceptual model of a gravity current in a thunderstorm outflow. There is a gust front at the nose of the current. The head of the outflow lifts the warm air mass and it causes a strong updraft. Kelvin-Helmholtz instability can be seen behind the head. In general, when the front of a thunderstorm outflow passes, the meteorological events on the ground are: (1) a sudden change of wind direction, (2) a sudden gust of wind, (3) a jump of air pressure, and (4) a sudden drop in temperature.

We assume that the northeasterly wind observed in the band cloud was a

gravity current. Because the wind direction suddenly shifted from NW to NE and the temperature dropped by about 1°C (as shown in Fig. 8) when the northeasterly flow arrived at the radar site. On the contrary, no gust was observed at that time. According to the detailed analysis of the raw data averaged in 10 seconds, just after the wind speed changed from 7.6 m/s at 0027 JST to 3.6 m/s at 0030 JST, sudden shifts of wind direction recovered at 0032 JST. It is considered that this phenomenon occurred when the stagnation point, which existed just ahead of the nose, passed the radar site. At the same time, the increase of air pressure was observed on the observation site (not shown), though it was not as large as that of ordinary gust front case.

The propagation speed of a gravity current U is calculated with the following equation (1) by Simpson (1987).

$$U=[Fr\ g\Delta z\{(P_2/P_1)T_1-T_2\}/T_2]^{\frac{1}{2}} \tag{1}$$

Here P_1, T_1, P_2, T_2, are air pressures and temperatures before (subscript 1) and after (subscript 2) the passage of a gravity current ; g is acceleration of gravity, Δz is the depth of a gravity current and Fr is a Freud number. By that $T_1-T_2=1$K, $\Delta z=1000$ m, $Fr=1$ and the pressure change by the passage of a front is negligible. The propagation speed U is estimated to be about 6 m/s for the case of the present analysis. This value corresponds well with the observed data. It is concluded that the cold northeasterly flow in the band cloud had the same structure as a gravity current, though a significant gust front was not observed there.

As was described in Fig. 11, rotors accompanied by weak echoes were shown in the rear of the head of the northeasterly flow in the band cloud. They are considered to be generated by Kelvin-Helmholtz instability. The K-H instability is generated under a state of a strong shear instability, i.e. Richardson number calculated with the following equation (2) is less than 0.25.

$$R_i=\frac{g}{\theta}\left(\frac{\Delta\theta}{\Delta z}\right)/\left(\frac{\Delta u}{\Delta z}\right)^2 \tag{2}$$

We calculated the Richardson number in the vertical cross section perpendicular to the approaching echoes (azimuth was 93.3° from north) at 2259 JST on January 22. Two dimensionality is assumed on this plane in the same way as the analysis of Fig. 10 and of Fig. 11. Then around the shear layer (within the height of 500-1500 m) such as shown in Fig. 11, $\Delta z=1000$ m, $\Delta u=0.61$ m/s, and we assumed $\Delta\theta=1$K and $g=9.8$ m/s^2. Therefore the R_i was calculated to be 0.243, which is less than the critical value of K-H instability. Moreover, the

vertical wind shear could be stronger in a realistic term because this plane was slightly different from the wind direction and the two dimensionality was assumed, as described before. The Richardson number may be smaller than this calculated value. Therefore the shear layer, within the height of 250-1250 m, met the state of K-H instability, and the waves which include rotors shown in Fig. 11 are considered to be K-H waves.

4.2 Thermodynamic structure of band cloud

From the soundings at Rebun Island and Wakkanai shown in Fig. 14, thermodynamic features of the vertical structure of the band cloud are estimated. At Rebun Island at 2000 JST, when a lot of open cell echoes were observed there, the depth of convective layer was estimated to be 1.9 km (below 780 mb). At Wakkanai at 2100 JST, when the band cloud was located there, and considered to be at a generating stage, the depth of mixing convective layer was estimated to be 2.7 km (below 700 mb). At a developed stage, that depth was considered to be deeper than 2.7 km. While the developed band clound was observed (from 2200 JST to 0300 JST), the eastern area of the shear line in the band cloud was covered with the cold northeasterly flow below 1.0 km. Therefore, it is estimated that there was a convectively stable layer below 1 km, a convectively unstable or a convectively neutral layer within the height of 1.0-2.7 km, and a convectively stable layer above 2.7 km. It is considered that the double inversion layers existed at the height of 1.0 km and 2.7 km in the east area of the shear line in the band cloud during the developed stage.

However, each of the inversion layers has a different characteristics. The upper one contributed thermodynamical instability to enhancing the convection of the clouds. On the contrary, the lower one contributed dynamical instability to the strong updraft along the horizontal shear line.

Such a vertical thermodynamic structure has the following similarity to band clouds generated over the western Japan Sea, analyzed by JMA (1988): (1) there were open cell convective clouds in the west (southwest) of the band cloud, (2) the eastern (northeastern) air was colder than the western (southwestern) air in the lower layer in the band cloud, (3) there were double inversions in the east (northeast) of the band cloud, (4) there was a strong vertical shear around the lower inversion layer in the band cloud. But there are a few differences between the two cases as well: (1) the wind shift observed at Rebun Island was much larger than that observed by JMA (1988), (2) the approaching direction of band cloud toward Rebun Island was different to both the northwesterly and northeasterly flows by nearly 45°, but the one observed by JMA (1988) was the

same as that of one main flow being comprised in the band cloud, (3) the band cloud weakened no sooner than the northeasterly flow stopped supplying from the Soya Strait, but the colder northerly wind observed by JMA (1988) was blowing continuously during the observation.

4.3 Generating and developing mechanism of northeasterly flow

In the conclusion of the present study, we made a conceptual model of the formation of the band cloud (Fig. 15). The generating and developing mechanism of the band cloud is considered as follows. There was a thermodynamically unstable layer below 2.7 km around Wakkanai. And a lot of isolated convective clouds were generated off the west coast of Hokkaido Island. Then the shallow northeasterly cold air intruded toward the west, and it forcibly enhanced cumulus convections. The band cloud was generated along the horizontal shear line which was between the northeasterly flow and northwesterly winter monsoon. There was a strong vertical shear around the lower inversion layer (1.0 km).

Then we discuss the formation of the cold northeasterly flow. Nagata and Ikawa (1988) suggested that a cold air mass which originates over Siberia disperses over Sakhalin. One air mass flows over the Okhotsk Sea, and the other flows over Japan Sea. Usually there are lot of drift ices around the Sakhalin Island on the Okhotsk Sea in the winter. The air is transferred less sensible heat over the drift ices than the unfrozen sea. This thermal contrast

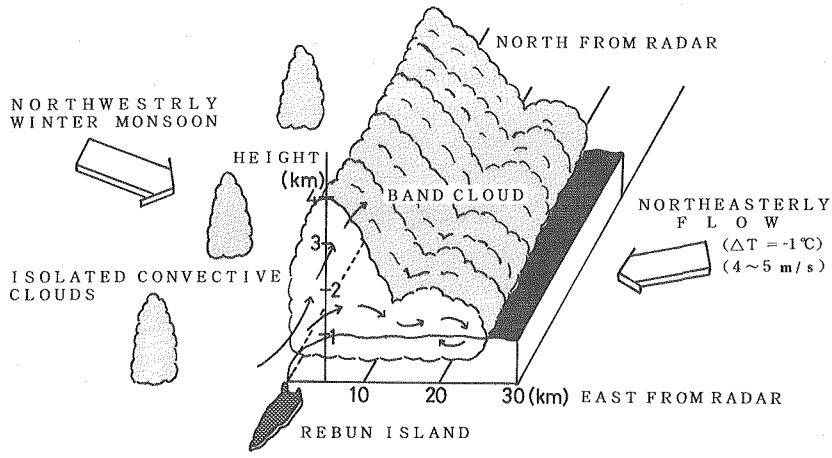

Fig. 15. Schematic illustration of conceptual model of the band cloud. A bird's eye view from southeast shows radar echo image and internal flow of the band cloud.

results in generating the shallow cold flow.

In our study, there was the center of a very cold air mass (below −24°C) at 850 hPa over Sakhalin at 2100 JST on January 22. The direction of contours at 850 hPa over Sakhalin was northwest (NW)-southeast (SE) at 2100 JST on January 20. It changed to north-northwest (NNW)-south-southeast (SSE) at 2100 JST on January 21. Then it changed to NW-SE again at 0900 JST on January 23. This synoptic scale condition made the air in the lower level (below 1.5 km) nearby the east of the Okhotsk Sea easier to penetrate into the Japan Sea through the Soya Strait during EVENT2 (the period when the band cloud was observed).

Fujiyoshi et al. (1994) studied the formation of a northeasterly wind by making simultaneous observations at Rebun Island and the Soya Cape in Wakkanai City. They considered the speed of wind after flowing through the Soya Strait from the Okhotsk Sea, was higher than that of northerly wind, which flew from the west of Sakhalin, because the area of the outlet was smaller than that of the inlet. In our study, the shallow colder flow blowing from the Okhotsk Sea was enhanced by the topographic effect after flowing through the Soya Strait. Both the enhancement of the northeasterly flow and the difference of temperature between northwesterly and northeasterly flows played an important role on generating a gravity current.

On the 850 hPa isobalic surface, by 0900 JST on January 23, the direction of contour over Hokkaido Island and Sakhalin had changed from NNW-SSE to NW-SE, the equivalent potential temperature over Wakkanai had increased (Fig. 3(a)) as well as the temperature over Sakhalin had increased (by about 2°C by 2100 JST on January 23). As a consequence of this change of synoptic scale condition, the penetration of air, which had flown through the Soya Strait from the Okhotsk Sea to the Japan Sea, stopped after 0300 JST January 23. This change of wind is assured from the ground data at Wakkanai (Fig. 8). The wind shifted from NE at a speed of 4-5 m/s to weak wind (N at 1 m/s) there at 0300 JST, though the temperature dropped by 2°C since it was begun prevailed by the air from inland Hokkaido.

The band cloud was strongly affected by this dissipation of northeasterly flow. Convective cells weakened since the shallow cold air had stopped supplying. The horizontal shear line got obscured and was dissipated after 0300 JST on January 23. The band cloud started receding and weakening simultaneously. Finally the observation site (Rebun Island) was prevailed by the northwesterly monsoon.

5. Conclusions

Observations were carried out in Rebun Island with dual-linear-polarization Doppler radar and radiosonde etc. from January 16 to 28, 1991. Four snow falling events were observed during this observation period. Many convective clouds in winter monsoon surges were observed hardly affected by orographic effects. A long-lasting broad band cloud was observed within the range of the Doppler Radar from January 22 to 23 (EVENT2). The band cloud was generated at about 2100 JST on January 22 around the Soya strait. Then the band cloud was developed as it proceeded southwest. The band cloud was more than 100 km in length and more than 20 km in width at the mature stage. At about 0030 JST, the head of the northeasterly flow reached the rader site (Rebun), after staying around Rebun Island in a steady state for about 2 hours, it receded east and weakened. When a very strong echo covered the observation site, soft hails were observed, and rimed snowflakes were observed when echoes were weakened. Just after the head of the band cloud passed the radar site, the temperature decreased about 1°C and the wind direction shifted from strong northwesterly (7 m/s) to weak northeasterly (4 m/s) drastically. The temperature and wind from 0030 JST to 0320 JST in Rebun Island was nearly equal to that in Wakkanai.

The internal kinematic structures of the band clound was analyzed in detail. The band cloud was generated along the horizontal shear line between a northeasterly flow blowing from the Soya Strait and the northwesterly monsoon over the west of the Soya Strait. Strong convective cells lined up regularly at the interval of about 4 km along the shear line. The maximum height of these echoes reached up to 4 km. These echoes inclined to the west (to the up shear side). The northwesterly wind was lifted at the head of the easterly wind, and a strong updraft, which was up to 5 m/s was generated there due to the strong horizontal convergence. There was an strong vertical wind shear at an altitude of about 1 km around the boundary between these two flows. We assume that some of the rimed snowflakes grew into the soft hail just behind (east of) the updraft, and the other ones were transferred backward (to the east) further than the soft hails due to the light weight.

Dynamic structure of the northeasterly flow is discussed. We find out that the northeasterly flow in the band cloud have the same structure as a gravity current. The thermodynamic structure in the band cloud is analyzed with the soundings at Rebun Island and Wakkanai. The formation and developing mechanisms of the band cloud, and the formation mechanism of northeasterly

flow are discussed comprehensively.

The present case study suggested the importance of the cloud and shallow northeasterly flow for the formation and maintenance of the band cloud, though further investigations are required for the general understanding of the phenomena and for giving a better name to the band cloud.

Acknowledgments

The authors express their thanks to Dr. N. Takahashi and the students of Meteorological Laboratory, Hokkaido University for their assistance in the observation, to the Rebun Town Hall for their cooperation and providing for installations and facilities, and to Japan Meteorological Agency for permission to use meteorological data. NOAA data was recorded by the Research Center for Atmospheric and Oceanic Variations, Tohoku University. The authors express their thanks to Prof. Hiroshi Kawamura, Tohoku University for providing the NOAA data. The authors extend their thanks to Mr. Iori Tanaka, Hokkaido Central Fisheries Experimental Station for providing the sea surface temperature data. The expense of this study was supported by the Grant-in-Aid for Scientific Research of the Ministry of Education, Science, Sports and Culture of Japan. This study was partly supported by the Research Development Fund of Foundation of River and Basin Integrated Communication, Japan.

References

Browning, K.A and R.Wexler, 1968. The determination of kinematic properties of a wind field using Doppler radar. J. Appl. Meteor., **7**, 105-113.

Fujiyoshi, Y., Y. Kodama, K. Tsuboki, K. Nishimura and N. Ono, 1996. Structure of a cold air during the development of a broad band cloud and meso-β-scale vortex : Simultaneous two-point radiosonde observations. J. Meteor. Soc. Japan, **74**, 281-297.

Ishihara, M., H. Sakakibara and Z. Yanagisawa, 1989. Doppler radar analysis of the structure of mesoscale snow bands developed between the winter monsoon and the land breeze. J. Meteror. Soc. Japan, **67**, 503-520.

Kibe, S., 1988. Small scale low in the vicinity of the west coast of Hokkaido Island. Tenki, **35**, 146-151. (in Japanese).

Kobayashi, F., K. Kikuchi and T. Motoki, 1987. Studies on the convergence band clouds formed in the mid-winter seasons on the west coast of Hokkaido Island, Japan (I). Geophys. Bull. Hokkaido Univ., **49**, 341-357. (in Japanese with English abstract).

Koscienlny, A.J., R.J. Doviak and R. Rabin, 1982. Statistical considerations in the estimation of divergence from single-Doppler radar and application to prestorm boundary-layer observations. J. Appl. Meteor., **21** 197-210.

Nagata, M., 1992. Modeling case study of the Japan-Sea convergent cloud band in a varying large-scale environment: Evolution and upscale effect. J. Meteor. Soc. Japan, **70**,

649-671.

Nagata, M., 1993. Meso-β-scale vortices developing along the Japan-Sea Polar-airmass Convergence Zone (JPCZ) cloud band: Numerical simulation. J. Meteor. Soc. Japan, **71**, 43-57.

Nagata, M. and M. Ikawa, 1988. Numerical experiments of the convergence band cloud over Japan Sea. Tenki, **35**, 151-155. (in Japanese).

Nagata, M., M. Ikawa, S. Yoshizumi and T. Yoshida, 1986. On the formation of a convergence cloud band over the Japan Sea in winter; Numerical experiments. J. Meteor. Soc. Japan, **64**, 841-855.

Ninomiya, K., K. Wakahara and H. Ohkubo, 1993. Meso-α-scale low development over the northeastern Japan Sea under the influence of a parent large-scale low and a cold vortex aloft. J. Meteor. Soc. Japan, **71**, 73-91.

Okabayashi, T. and M. Satomi, 1971. A study on the snowfall and its original clouds by meteorological rader and satellite (part I). Tenki, **18**, 573-581. (in Japanese).

Research Group on Mesoscale Meteorology of Marine Department, JMA, 1988. On the mesoscale structure of the cloud band over Japan Sea in winter monsoon period. —A mesoscale observation on board R/V Keifu-Maru. Tenki, **35**, 237-248 (in Japanese).

Simpson, J.E., 1987. Gravity currents in the environment and the laboratory. Ellis Horwood Limited, 244pp.

Tsuboki, K., Y. Fujiyoshi and G. Wakahama, 1989. Doppler radar observation of convergence band cloud formed on the west coast of Hokkaido Island. II: Cold frontal type. J. Metor. Soc. Japan, **67**, 985-999.

Tsuboki, K. and G. Wakahama, 1988. Single Doppler radar measurements of a kinematic wind field: VAD analysis based on a least-squares-fitting method. Low Temperature Science, Ser. **A47** (with English summary 87pp.).

Tsuboki, K. and G. Wakahama, 1992. Mesoscale cyclogenesis in winter monsoon air streams: Quasi-geostrophic baroclinic instability as a mechanism of the cyclogenesis off the west coast of Hokkaido Island, Japan. J. Meteor. Soc. Japan, **70**, 77-93.

Uyeda, H., R. Shirooka, K. Iwanami, A. Takemoto, K. Kikuchi, G. Yoshida and M. Okazaki, 1991. Observation of vertical structures of convective snow clouds with a dual-polarization radar in Hokkaido, Japan. Preprints, 25th International Conference on Radar Meteor., Paris, 717-719.

Waldteufel, P. and H. Corbin, 1979. On the analysis of single-Doppler radar data. J. Appl. Meteor., **18**, 532-542.